



Flame synthesis and characterization of nanocrystalline titania powders

Bhaskaran Manjith Kumar, Subramshu Shekar Bhattacharya*

Nano Functional Materials Technology Centre, Material Testing Facility, Department of Metallurgical & Materials Engineering, Indian Institute of Technology Madras, Chennai – 600 036, India

Received 15 May 2012; received in revised form 12 September 2012; accepted 21 September 2012

Abstract

Flame reactors are considered to be one of the most promising and versatile synthesis routes for the large-scale production of submicron and nanosized particles. An annular co-flow type oxy-gas diffusion burner was designed for its application in a modular flame reactor for the synthesis of nanocrystalline oxide ceramics. The burner consisted of multiple ports for the individually regulated flow of a precursor vapour, inert gas, fuel gas and oxidizer. The nanopowders formed during flame synthesis in the reaction chamber were collected by a suitable set of filters. In the present study, TTIP was used as the precursor for the synthesis of nanocrystalline TiO₂ and helium was used to carry the precursor vapour to the burner head. Methane and oxygen were used as fuel and oxidizer respectively. The operating conditions were varied by systematically changing the flow rates of the gases involved. The synthesized powders were characterized using standard techniques such as XRD, SEM, TEM, BET etc., in order to determine the crystallite size, phase content, morphology, particle size and degree of agglomeration. The influences of gas flow rates on the powder characteristics are discussed.

Keywords: *nanocrystalline titania, flame synthesis, diffusion burner, aerosol flame reactor*

I. Introduction

The recent importance of nanomaterials with length scales well below 100 nm stem essentially from the ability to access properties that are otherwise not exhibited by the material in its conventional or bulk form. At such length scales a substantial proportion of the atoms reside on the surface and the volumes of interfaces as well as defects are significant, which result in interesting properties and, sometimes, non-equilibrium behaviour [1–5]. Nanomaterials are typically synthesised either by breaking down larger grained bulk materials in the top-down approach or built up from atomic/molecular precursors in the bottom-up approach.

In the bottom-up approach, nanomaterials are commonly synthesized by liquid phase or gas phase routes. Gas phase synthesis routes take advantage of the fact that the particles produced have better homogeneity and the process times are fairly short when compared to liquid phase synthesis methods [6,7]. A highly promising

gas phase processing technique for the production of nanocrystalline materials is the flame synthesis method which can be easily scaled-up to industrial levels without having to sacrifice control over the final product.

In flame synthesis, the energy required to drive the chemical reactions of the precursors is obtained from the flame. As a result of the decomposition/pyrolysis reaction at high temperatures in the flame, atomic clusters of the product are formed which further grow to nanoparticles by surface growth coagulation or coalescence [8]. The process parameters affect the flame characteristics which, in turn, decide the particle size, morphology and crystallinity. Hence the properties of the nanoparticles can be controlled by judicious manipulation of the process parameters [9]. The high temperature also helps in maintaining a self-purifying environment. High purity, low synthesis costs and high production rates, along with the flexibility in the production of a wide variety of nanocrystalline and/or nanostructured materials, makes flame synthesis an excellent choice among the gas phase synthesis routes [10].

* Corresponding author: tel: +91 44 22574765
fax: +91 44 22574752, e-mail: ssb@iitm.ac.in

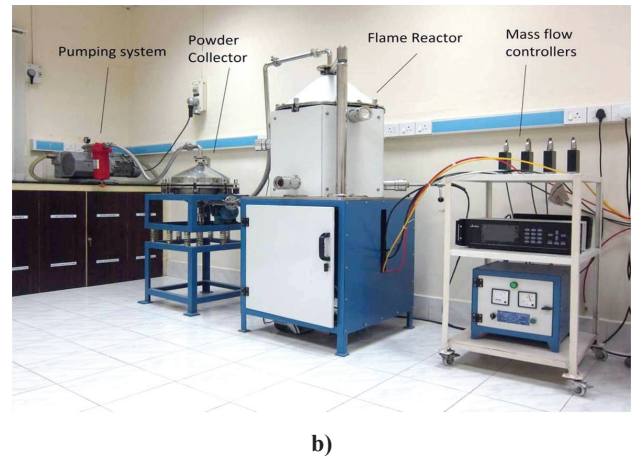
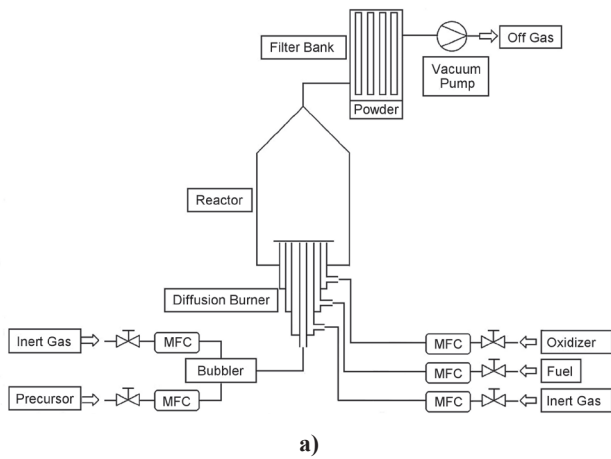


Figure 1. Schematic (a) and photograph (b) of the experimental set-up used in the flame synthesis of nanocrystalline TiO_2

Titanium dioxide (TiO_2) in the conventional form has found use in many applications. However, with the advent of nanoscience and technology, the potential of nanocrystalline TiO_2 as a functional material can be exploited further. It has been found that the functionality of nanostructured TiO_2 strongly depends on particle and crystallite size, morphology, degree of agglomeration and crystal structure [11,12]. Nano-crystalline TiO_2 is used in photo catalysis, solar cells, water and air purification, gas sensing and catalytic conversion.

Titania has three polymorphic forms, anatase, rutile and brookite. Out of these different forms, anatase titania has the highest photo-catalytic ability [13,14] and has hence been used extensively in decontamination treatment [15].

In this paper, synthesis of nanocrystalline titania, using a flame aerosol reactor, is described. The perfor-

mance of an indigenously fabricated flame reactor is demonstrated by synthesizing titania with reasonable control in the size, phase content and morphology.

II. Experimental

The modular flame reactor set-up primarily consisted of a precursor delivery system, multi-port diffusion burner within a reaction chamber, particle collection unit and vacuum generating system. A schematic flow diagram is shown in Fig. 1a and the actual photograph of the experimental set-up is given in Fig. 1b. In the present study, titanium tetra isopropoxide, TTIP (Alfa Aesar, purity 97%) was used as the precursor for the synthesis of nanocrystalline titania.

For the supply of precursor vapour to the burner and reaction chamber, TTIP was taken in a bubbler unit and placed in an oil bath maintained at a tem-

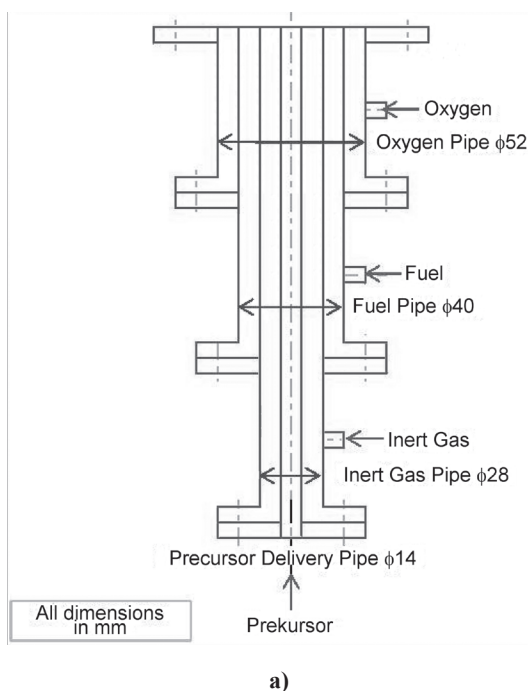


Figure 2. Schematic (a) and photograph (b) of the diffusion burner used in the flame synthesis

Table 1. Flow parameters used for flame synthesis of nanocrystalline titania

Helium flow [slm]				Oxygen flow [slm]				Methane flow [sccm]			
1	2	3	4	5	10	15	20	20	40	60	80

perature of 125 °C. Helium was used as a carrier gas to transport the precursor to the burner. Methane was used as the fuel for generating the flame along with oxygen. The flow rates of all the gases into the reaction chamber were precisely regulated using suitable thermal mass flow controllers (MKS make).

The reaction chamber was made from stainless steel capable of being hermetically sealed and provided with glass view-ports. The vertically positioned reaction chamber consisted of a multi-port co-flow diffusion burner at the bottom. A schematic of the diffusion burner is given in Fig. 2a and an actual photograph is presented in Fig. 2b. Figure 2a also gives the locations at which the different gases were admitted into the burner. The carrier gas with precursor vapour was passed through the central tube of the burner where it decomposed/pyrolysed and resulted in the production of titania particles. The present burner configuration enabled independent control of the flow rates of each gas.

For the establishment of a flame at the burner head, a spark generator was used by positioning an electrode directly over the burner head, which was retracted once the flame was established. The titania particles produced from the pyrolysis reaction of the TTIP in the flame [16–19] were trapped by the filter unit array in the particle collector unit. To maintain a constant flow of gases and reaction products from the reaction chamber to the particle collector unit, a vacuum pump (PVR make, 65 m³/min capacity) was used.

During the actual experimental studies, the precursor flow was started only after the flame had stabilised. Systematically varying gas flow rates as shown in Table 1 were used in this study for the synthesis of nanocrystalline titania.

After the conclusion of the experiment, the titania particles were collected from the filter and characterized. The crystallinity and phase of the titania particles were confirmed by X-ray diffraction, XRD (make Bruker D8) using Cu K α (1.54 Å) radiation. The anatase and rutile phase contents of the powder were calculated by analysing the intensities of anatase 101 peak at $2\theta = 25.5^\circ$ and rutile 110 peak at $2\theta = 27.5^\circ$. The anatase fraction (F_A) was found by the following equation [20]:

$$F_A = 100 - \frac{1}{1 + 0.8 \frac{I_A}{I_R}} 100 \quad (1)$$

where I_A is the intensity of the 101 peak of anatase and I_R is the intensity of the 110 peak of rutile.

The crystallite size L was calculated from the full width at half maximum (FWHM) of the anatase 101 peak using Scherrer’s formula:

$$L = K\lambda/(\beta \cos\theta) = d_{XRD} \quad (2)$$

where λ is the wavelength of X-ray used, K is 0.9 and β is the FWHM. The above method can be applied to calculate crystallite sizes well below 100 nm [21].

The specific surface area of the powder was measured by nitrogen adsorption following a BET (Brunauer–Emmett–Teller) approach. Assuming mono-disperse uniform particles, the average effective particle size d_{BET} was calculated using the formula:

$$d_{BET} = 6/S\rho \quad (3)$$

where S is the specific surface area and ρ is the theoretical density. Assuming that the crystallites and particles to be nearly spherical in shape, the degree of agglomeration N was found by the equation [18,19,22]:

$$N = \frac{d_{BET}^3}{d_{XRD}^3} \quad (4)$$

III. Results and discussion

The powders collected from the filter assembly of the particle collector unit were brilliant white in colour and very fluffy, suggesting a low degree of agglomeration. XRD analyses of the powders synthesised under all the processing conditions revealed them to be pure titania, predominantly in the anatase form. In some cases a small quantity of rutile could be discerned. The

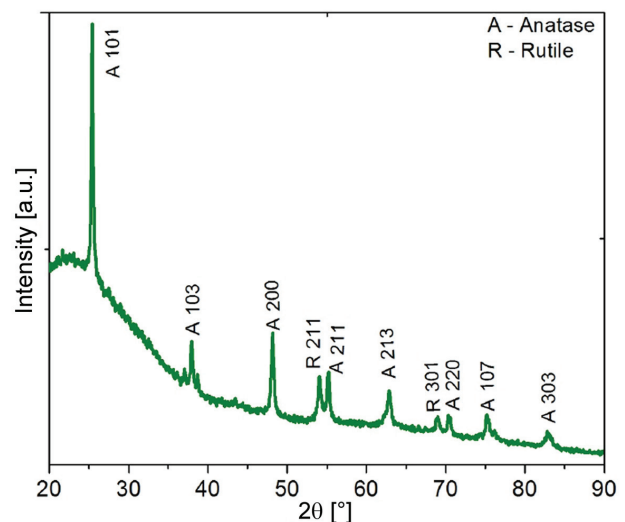
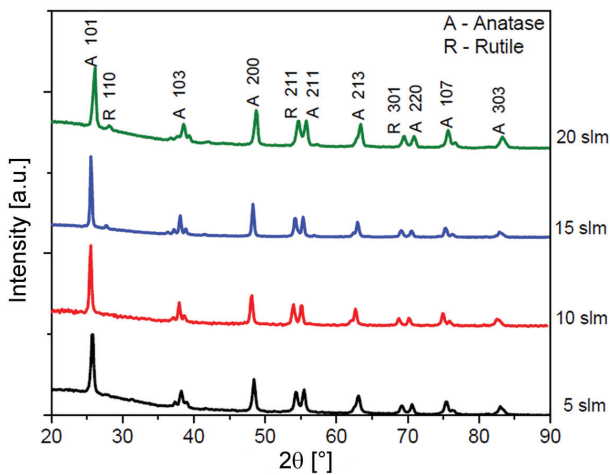
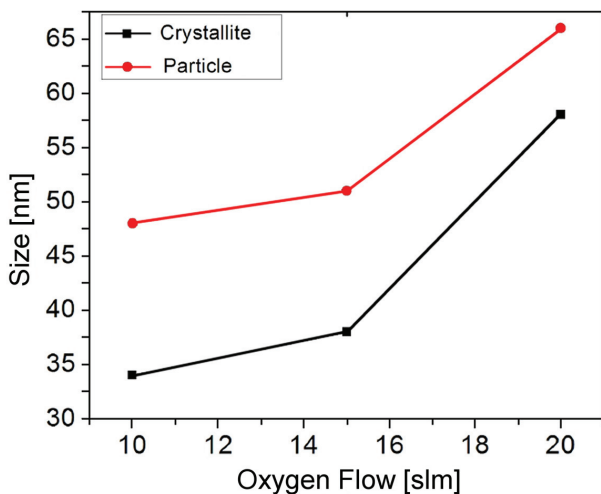


Figure 3. XRD pattern of nanocrystalline TiO₂ synthesised with flow rates of He at 2 slm, CH₄ at 40 sccm and O₂ at 10 slm

Table 2. Effect of varying flow parameters on particle size and degree of agglomeration in flame synthesis of nanocrystalline titania

He flow rate [slm]	O ₂ flow rate [slm]	Specific surface area [m ² /g]	d_{BET} [nm]	d_{XRD} [nm]	$N = d_{BET}^3/d_{XRD}^3$
1	10	30	53	38	2.7
2	10	32	48	34	2.8
3	10	60	26	16	4.2
4	10	116	16	10	4.1
1	15	26	62	50	1.9
2	15	31	51	38	2.4
3	15	50	32	21	3.5
4	15	100	19	12	3.9
1	20	24	66	58	1.4
2	20	29	55	46	1.7
3	20	37	43	30	2.9
4	20	90	21	14	3.3

**Figure 4. XRD patterns of nanocrystalline TiO₂ synthesised with He at 2 slm, CH₄ at 40 sccm and varying O₂ flow rates****Figure 5. Variation in size of nanocrystalline TiO₂ synthesised with He at 2 slm, CH₄ at 40 sccm and varying O₂ flow rates**

broad nature of the peaks in all the X-ray diffractograms suggested ultra-fine crystallite sizes in the nanometric range. An example is provided as Fig. 3 in case of the powder synthesised at He flow rate of 2 slm, CH₄ flow rate of 40 sccm and O₂ flow rate of 10 slm.

The crystallite sizes calculated from the XRD patterns and the specific surface areas obtained from the nitrogen adsorption studies are given in Table 2. From the comparable values of d_{BET} and d_{XRD} , it is quite evident that the synthesized powder is non-agglomerated in nature.

It can be seen that at constant carrier and fuel gas flow rates, an increase in the oxygen flow rate resulted in an increase in the rutile content of the powder. This is depicted in Fig. 4 where the carrier and fuel gas flow rates were maintained constant at 2 slm and 40 sccm respectively while the oxygen flow rate was systematically varied from 5 to 20 slm. The corresponding crystallite and particle sizes also increased when the oxygen flow rate was increased. On the other hand, the degree of agglomeration showed a reversed trend with increasing oxygen flow rate. The influence of increasing oxygen flow rate on the crystallite and particle size is depicted in Fig. 5.

Wegner and Pratsinis [23] and Sunsap *et al.* [24] found that the particle sizes reduced with increased oxygen flow rates while Maddler *et al.* [25] and Jang and Kim [26] reported that the particle sizes increased at oxygen flow rates greater than 3 slm. In the present study the trends in the particle and crystallite sizes were attributed to the increase in the flame temperature due to the higher oxygen flow rate. In non-equilibrium processes such as flame reactions, the oxygen requirement is well above the stoichiometric value and, in the present case, the flame is “fuel-rich”. Therefore, an increase in the oxygen flow rate resulted in a more oxidising environment, which led to a higher flame temperature. The higher temperatures subsequently resulted in

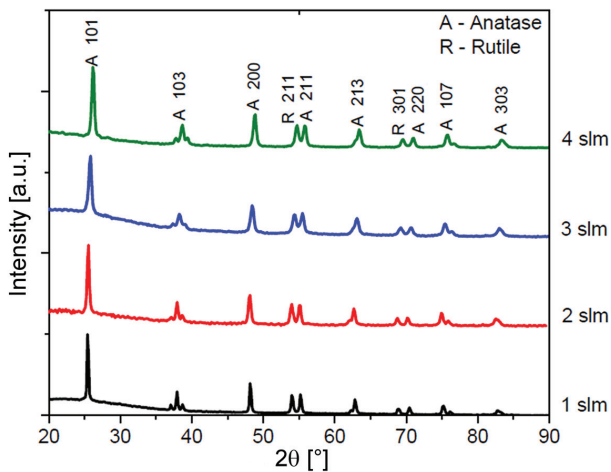


Figure 6. XRD patterns of nanocrystalline TiO₂ synthesised at a constant CH₄ flow rate of 40 sccm, O₂ flow rate of 10 slm under varying He flow rates

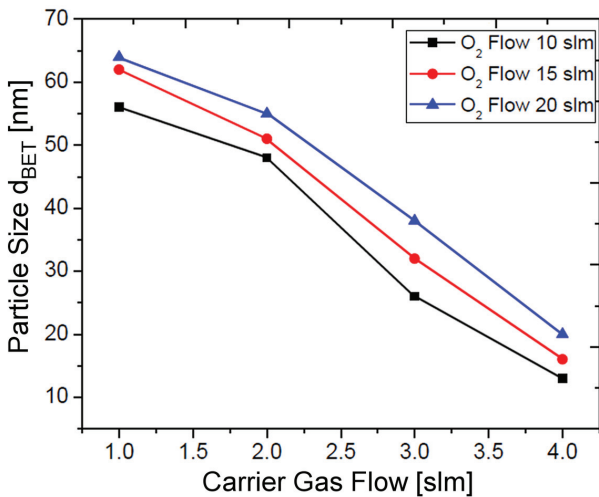
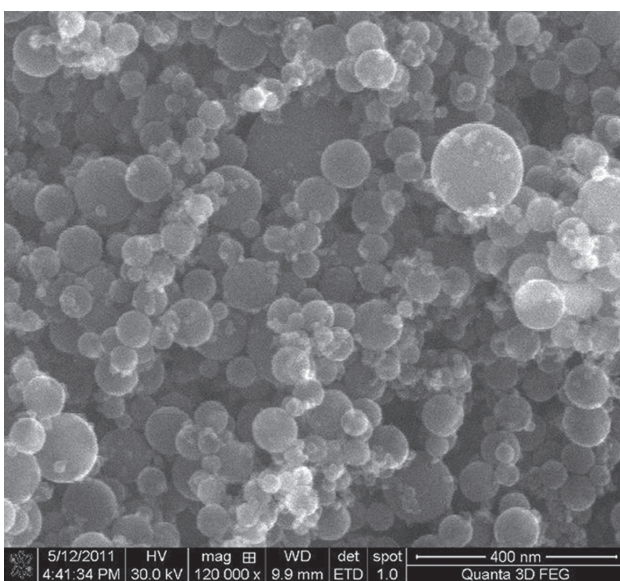
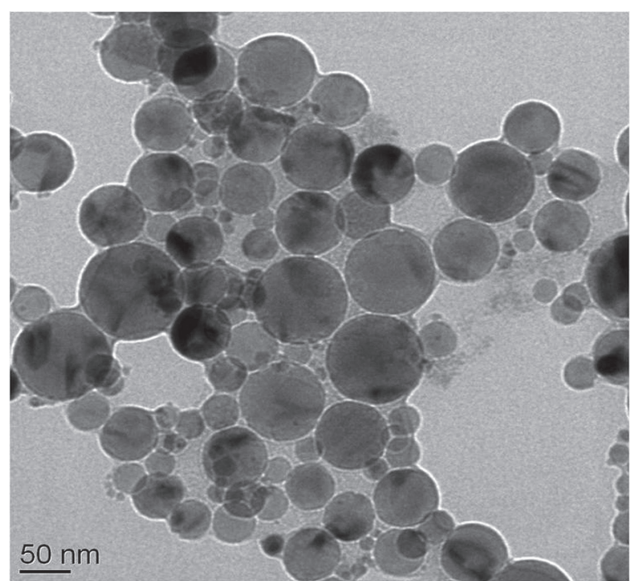


Figure 7. Variation of the particle size of nanocrystalline TiO₂ with carrier gas flow rate at different constant oxygen flow rates



a)



b)

Figure 8. SEM (a) and TEM (b) images of nanocrystalline TiO₂ synthesised with flow rates of He at 2slm, CH₄ at 40 sccm and O₂ at 10 slm

larger crystallite and particle sizes. However, the impact of an increase in temperature was greater on the crystallite size when compared to the particle size because particle growth required coagulation and sintering between separate particles whereas crystallite growth was easily favoured within a particle (which is composed of crystallites in direct contact with each other). Hence, the degree of agglomeration dropped marginally as the temperature increased. This is evident from Fig. 5 as the difference between the particle size and the crystallite size progressively reduced with increase in oxygen flow rate. In addition, the higher temperatures favoured the anatase to rutile transformation and so, the rutile content increased with increasing oxygen flow rates.

An increase in the carrier gas flow rate at constant fuel and oxygen gas flow rates resulted in a decrease in the crystallite and particle sizes, but marginal increase in degree of agglomeration. Figure 6 shows the diffractograms of TiO₂, synthesized at constant methane flow rate of 40 sccm and oxidizer flow rate of 10 slm with the carrier gas (He) flow rates varying from 1 to 4 slm.

The observed trends in the crystallite and particle sizes were explained in terms of the residence time of the particle within the flame. Although an increase in the carrier gas flow rate led to an increase in the concentration of the precursor, it also resulted in a significant decrease in the residence time of the particles in the flame. This decrease in the residence time suppressed both crystallite and particle growth and as a result, smaller sizes were obtained. On the other hand, the increased concentration of the precursor with increasing carrier gas flow rate led to the generation of a greater number of primary particles of titania in the flame. This, in turn, resulted in more collisions and contact between the primary particles and increased the possibility of forming soft and hard agglom-

Table 3. Mean particle size and standard deviation of flame synthesized nanocrystalline titania

He flow rate [slm]	CH ₄ flow rate [sccm]	O ₂ flow rate [slm]	Geo. mean diameter [nm]	Geo. standard deviation
1	40	10	49	1.006
2	40	10	44	1.032
3	40	10	23	1.018
4	40	10	17	1.102
1	40	20	60	1.121
2	40	20	51	1.001
3	40	20	37	1.048
4	40	20	19	1.021

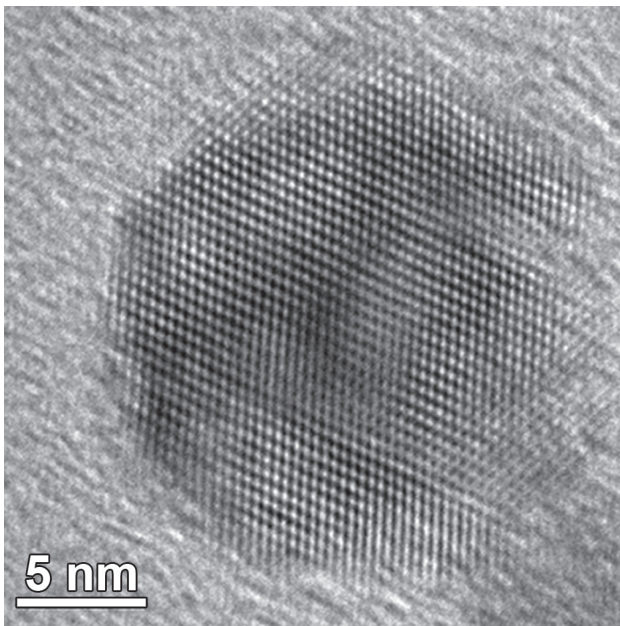


Figure 9. HRTEM image of nanocrystalline TiO₂ synthesised with flow rates of He at 3 slm, CH₄ at 40 sccm and O₂ at 10 slm

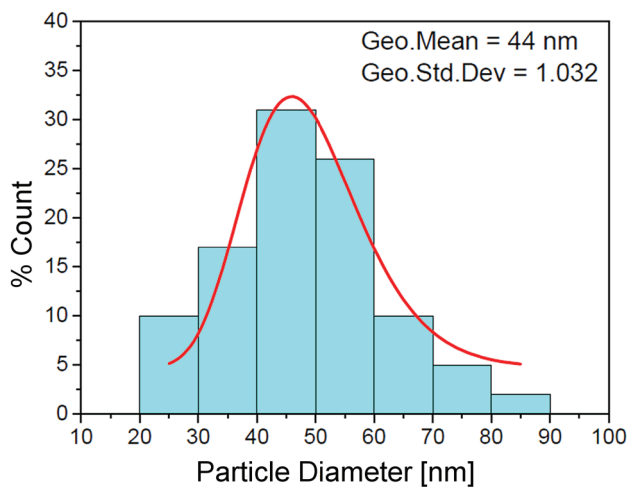


Figure 10. Particle size distribution of nanocrystalline TiO₂ synthesised with flow rates of He at 2 slm, CH₄ at 40 sccm and O₂ at 10 slm

erates through coagulation. However, the decrease in the residence time offset the possibility of forming larger particles through complete sintering and hence the degree of agglomeration increased marginally with increase in the carrier gas flow rate. The variation of the particle size as a function of the carrier gas flow rate at three different oxygen flow rates is depicted in Fig. 7.

The morphology of the as-synthesized TiO₂ particles was found to be completely spherical in case of all the processing conditions. An example is presented as Fig. 8a in the form of an SEM image (FEI Quanta 3D). Although some light aggregates of the smaller spherical particles can be seen, most of the particles are of reably uniform size. It is well known that temperature, residence time and reaction kinetics affect the particle morphology during flame synthesis. In general, if the rate of sintering or coalescence of particles is slower than the rate of collision of particles, then agglomerated particles are formed. On the other hand, if the sintering or coalescence rate is faster than the rate of collisions, then regularly shaped spherical particles are formed [27–29].

For detailed analysis of the particle size, morphology and size distribution, transmission electron microscopy (FEI Technai 20F) was carried out. The TEM images confirmed the ultra-fine sizes, spherical morphology and non-agglomerated nature of the powders (see, for example, Fig. 8b). A high resolution TEM image of a particle (Fig. 9) reveals the presence of lattice fringes right up to the edge of the particle indicating a high degree of crystallinity and absence of any amorphous content.

Histograms describing the particle size distributions of the as-synthesized TiO₂ powders were made from TEM images. For each of the histograms a distribution function was “fitted” which gave an idea of the type of distribution. For the powder synthesized at a He flow rate of 2 slm, methane flow rate of 40 sccm and oxygen flow rate of 10 slm, the particle distribution histogram is given in Fig. 10. It can be seen that the size distribution is mono-modal, fairly narrow and follows a lognormal pattern. Table 3 gives the mean particle size and standard deviations of the powders synthesized under different processing conditions.

IV. Conclusions

A modular and versatile flame reactor set-up was developed for the controlled production of nanocrystalline ceramic oxides. Synthesis of nanocrystalline TiO₂ powder was successfully carried out by the oxidation/decomposition/pyrolysis of a metal organic precursor, TTIP. The as-synthesised powders were found to be predominantly in the anatase form with little or no rutile content. By systematically varying the process parameters such as carrier gas and oxygen flow rates, a fair degree of the control could be established on the rutile content, crystallite size, particle size and the degree of agglomeration in the final product. In all the cases studied, the as-synthesised nanoparticles were found to have a spherical morphology with a fairly narrow size distribution.

Acknowledgement: The financial support by the DST, India to establish a Nano Functional Materials Technology Centre at IIT Madras, under which this work was carried out, is gratefully acknowledged.

References

- O. Preining, "The physical nature of very, very small particles and its impact on their behavior", *J. Aerosol Sci.*, **29** [5] (1998) 481–495.
- R.W. Siegel, "Nanophase materials assembled from atom clusters", *Mater. Sci. Eng. B*, **19** [2] (1993) 37–43.
- H. Hahn, H. Hasemann, W. Epling, G.B. Hoflund, "Comparison of nanocrystalline and poly crystalline oxide supports for catalytic oxidation of methane", *Mater. Res. Soc. Symp.*, **497** (1997) 35.
- F.E. Kruis, H. Fissan, A. Peled, "Synthesis of nanoparticles in the gas phase for electronic, optical and magnetic applications - A review", *J. Aerosol Sci.*, **29** [5] (1998) 511–535.
- C. Wang, S.K. Friedlander, L. Madler, "Nanoparticle aerosol science and technology: An overview", *China Particuology*, **3** [5] (2005) 243–254.
- H.K. Kammler, L. Madler, S.E. Pratsinis, "Flame synthesis of nanoparticles", *Chem. Eng. Technol.*, **24** [6] (2001) 583–596.
- T.T. Kodas, J.H. Mark, *Aerosol Processing of Materials*, Wiley-VCH, New York, 1999.
- K. Wegner, W.J. Stark, S.E. Pratsinis, "Flame nozzle synthesis of nanoparticles with closely controlled size, morphology and crystallinity", *Mater. Lett.*, **55** [5] (2002) 318–321.
- W.J. Stark, S.E. Pratsinis, "Aerosol flame reactors for manufacture of nanoparticles", *Powder Technol.*, **126** [2] (2002) 103–108.
- K. Wegner, S.E. Pratsinis, "Scale up of nanoparticle synthesis in diffusion flame reactors", *Chem. Eng. Sci.*, **58** [20] (2003) 4581–4589.
- C.B. Almquist, P. Biswas, "Role of synthesis method and particle size of nanostructured TiO₂ on its photo activity", *J. Catalysis*, **212** [2] (2002) 145–156.
- D.R. Zhou, P. Biswas, J. Oostens, P. Boolchand, "Super conducting properties of aerosol generated YBa₂CuO_{7-δ} powders", *J. Am. Ceram. Soc.*, **76** [3] (1993) 678–682.
- P.H. Borse, L.S. Kankate, F. Dussenoy, W. Vogel, J. Urban, S.K. Kulkarni, "Synthesis and investigations of rutile phase of nanoparticles of TiO₂", *J. Mater. Sci.: Mater. Electron.*, **13** [9] (2002) 553–559.
- M.A. Fox, M.T. Dulay, "Heterogeneous photo catalysis", *Chem. Rev.*, **93** [1] (1993) 341–357.
- L. Znaidi, R. Seraphimova, J.F. Boiquet, C. Colbean, C. Pommier, "A semi continuous process for the synthesis of nanosize TiO₂ powder and their use as photo catalysts", *Mater. Res. Bull.*, **36** [6] (2001) 811–825.
- K.K. Akurati, S.S. Bhattacharya, M. Winterer, H. Hahn, "Synthesis, characterisation and sintering of nanocrystalline titania powder produced by chemical vapour synthesis", *Phys. D: Appl. Phys.*, **39** [10] (2006) 2248–2254.
- S. Seifried, M. Winterer, H. Hahn, "Nanocrystalline titania films and particles by chemical vapour synthesis", *Chem. Vap. Deposition*, **6** [5] (2000) 239–244.
- S. Klein, M. Winterer, H. Hahn, "Reduced pressure chemical vapour synthesis of nanocrystalline silicon carbide powder", *Chem. Vap. Deposition*, **4** [4] (1998) 143–149.
- M. Winterer, *Nanocrystalline Ceramics: Synthesis and Structure*, Springer, Berlin, 2002.
- R.A. Spurr, H. Myers, "Quantitative analysis of anatase-rutile mixtures with an X-ray diffractometer", *Analy. Chem.*, **29** [5] (1957) 760–762.
- B.D. Cullity, *Elements of X-ray Diffraction* 2nd ed., Addison-Wesley, Massachusetts, 1978.
- H.I. Hsiang, S.C. Lin, "Effects of aging on nanocrystalline anatase to rutile phase transformation kinetics", *Ceram. Int.*, **34** (2008) 557–561.
- K. Wegner, S.E. Pratsinis, "Gas phase synthesis of nanoparticles: Scale up and design of flame reactors," *Powder Technol.*, **150** [2] (2005) 117–122.
- P. Sunsap, D.J. Kim, K.S. Kim, "Characterization of TiO₂ particles synthesized in diffusion flame reactor", *Ind. Eng. Chem. Res.*, **47** [7] (2008) 2308–2313.
- L. Maddler, H.K. Kammler, R. Muller, S.E. Pratsinis, "Controlled synthesis of nanostructured particles by flame spray pyrolysis", *J. Aerosol Sci.*, **33** [2] (2002) 369–389.
- H.D. Jang, S.K. Kim, "Controlled synthesis of titanium dioxide nanoparticles in a modified diffusion flame reactor," *Mater. Res. Bull.*, **36**[4] (2001) 627–637.
- G.D. Ulrich, N.S. Subramanian, "Particle growth in flames: Coalescence as a rate controlling process", *Combustion Sci. Technol.*, **17** [4] (1977) 119–126.
- W. Koch, S.K. Friedlander, "The effect of particle coalescence on the surface area of a coagulating aerosol", *J. Colloid Interface Sci.*, **140** [2] (1990) 419–427.
- K.E.J. Lehtinen, R.S. Windeler, S.K. Friedlander, "Prediction of nanoparticle size and the onset of dendrite formation using the method of characteristic times", *J. Aerosol Sci.*, **27** [6] (1996) 883–886.

